Biogeosciences
Discussions

Open Access

Effects of heat and drought on carbon and water dynamics in a regenerating semi-arid pine forest: a combined experimental and modeling approach

N. K. Ruehr[1], B. E. Law[2], D. Quandt[2], and M. Williams[3]

[1]Karlsruhe Institute of Technology, Institute of Meteorology and Climatology – Institute of Atmospheric Environmental Research, 82467 Garmisch-Partenkirchen, Germany
[2]Oregon State University, College of Forestry, Department of Forest Ecosystems and Society, Corvallis, OR 97331, USA
[3]University of Edinburgh, School of GeoSciences, Edinburgh EH9 3JN, UK

Correspondence to: N. K. Ruehr (nadine.ruehr@kit.edu)

Title Page

Abstract	Introduction
Conclusions	References
Tables	Figures

|◀| ▶|
|◀| ▶|

Back | Close

Full Screen / Esc

Printer-friendly Version

Interactive Discussion

Abstract

Increasing summer temperatures and a reduction in precipitation will enhance drought stress in Mediterranean and semi-arid ecosystems. Predicting the net effects on forests' carbon and water balance will depend on our ability to disentangle the sensitivity of component fluxes responding to increasing soil and atmospheric drought. Here we studied carbon and water dynamics in a semi-arid regenerating ponderosa pine forest using field observations and process based modeling. Field observations of two summer dry seasons were used to calibrate a soil-plant-atmosphere (SPA) model. In addition, the ecosystem's response to reduced soil drought was quantified based on a field watering experiment and evaluated with the model. Further, the SPA model was used to estimate the relative effects of increasing soil and atmospheric drought over time, by simulating temperature and precipitation scenarios for 2040 and 2080.

The seasonality and drought response of ecosystem fluxes was well captured by the calibrated SPA model. Dramatic increases in summer water availability during seasonal drought had a small effect on pine physiology in both the watering experiment and the model. This clearly demonstrates that atmospheric drought induced a strong limitation on carbon uptake in young ponderosa pine due to tight regulation of stomatal conductance. Moreover, simulations showed that net ecosystem exchange (NEE) and gross primary productivity (GPP) were about three times more affected by summer heat and increased evaporative demand than by reductions in summer precipitation. Annual NEE decreased by 38 % in response to extreme summer conditions as predicted to occur in 2080 (June–August: +4.5 °C), because of a strong decline in GPP (-17 %) while heterotrophic respiration was relatively unaffected (-1 %). Considering warming trends across all seasons (September–May: +3 °C and June–August: +4.5 °C), the negative drought effects were largely compensated by an earlier initiation of favorable growing conditions and bud break, enhancing early season GPP and needle biomass. An adverse effect, triggered by changes in early season allocation patterns, was the decline of wood and root biomass. This imbalance may increase water stress over the

long-term to a threshold at which ponderosa pine may not survive, and highlights the need for an integrated process understanding of the combined effects of trends and extremes.

1 Introduction

⁵ Drought events are characterized by a continuous decline of soil water content (soil drought) and an increase in evaporative demand (atmospheric drought). The intensity of ecosystem water stress depends therefore largely on the initial soil water status, the length of the drought period and air temperature. The severity of summer droughts is increasing in the Northwest US (Easterling et al., 2007; Schwalm et al., 2012), due to

¹⁰ higher temperatures and a likely reduction in summer precipitation (Mote et al., 2013). However, our ability to predict future effects on forest ecosystems is limited by uncertainty regarding the relative roles of evaporative demand/temperature and precipitation in triggering drought stress (Williams et al., 2013), and by understanding their corresponding effects on component processes like photosynthesis and heterotrophic

¹⁵ respiration (Ruehr et al., 2012). For example, gross primary productivity is generally found to decrease more than respiration during drought conditions (Schwalm et al., 2009; Ruehr et al., 2012), because photosynthesis is limited by both soil drought and high temperatures, while soil moisture constraints on heterotrophic respiration may be partially compensated by temperature.

²⁰ Model predictions of drought impacts on the C cycle of forest ecosystems are further challenged by differences in site conditions that influence the intensity of stress experienced by the ecosystem (e.g., Wright et al., 2013). Moreover, tree adaptation strategies can affect the relative physiological sensitivity to evaporative demand and soil water availability. For example, isohydric pine close stomata early during water stress when

²⁵ vapor pressure deficit is large (Martinez-Vilalta et al., 2004) to avoid xylem cavitation (McDowell et al., 2008). In contrast, anisohydric juniper are less sensitive and can allow leaf water potentials to decline strongly while stomata remain open to continue

photosynthesis (McDowell et al., 2008). Because of a plethora of abiotic and biotic factors involved buffering and/or facilitating water stress, detailed site and species specific studies on drought stress are necessary to identify thresholds and increase process understanding.

Ponderosa pine (*Pinus ponderosa* Dougl. ex Laws.) represents a major forest type in semi-arid and Mediterranean climate zones in the Northwest US. The abundance of young, planted or naturally regenerating pine forests may increase, due to harvest and stand-replacing fires (Hudiburg et al., 2013; Pierce et al., 2004). However, young forest stands are more susceptible to water stress (Hanson and Weltzin, 2000; Irvine et al., 2004), due to shallower rooting (Williams et al., 2001) and a high vulnerability of the hydraulic system (Domec et al., 2004). Thus, the sensitivity of young ponderosa pine trees to increasingly extreme summer conditions may be considered a bottleneck in estimating the future distribution and productivity of this forest type.

Detailed process and site specific models can be used to test the sensitivity of component ecosystem fluxes and pools to changes in precipitation and temperature. Such a model of the soil-plant-atmosphere continuum has been developed by Williams et al. (1996). The SPA model estimates carbon and water fluxes at fine temporal scales within the limits of the hydraulic system and includes a detailed multi-layer soil and canopy model. The model's drought routine has been extensively tested in a variety of ecosystems world-wide (e.g., Williams et al., 2001; Fisher et al., 2007; Zeppel et al., 2008; Wright et al., 2013). Stomatal conductance is linked to the Farquahr model of leaf-level photosynthesis and the Penman–Monteith equation of leaf-level transpiration to optimize carbon gain per unit leaf nitrogen within the limitations of the hydraulic system. Maximum soil-to-canopy water transport is defined by the difference between soil water potential and the minimum sustainable leaf water potential, and by the hydraulic resistance of the soil-root-leaf pathway. The risk of cavitation is then limited by stomata adjusting to equalize evaporative losses with water supply. To determine net ecosystem exchange, respiratory fluxes, growth and litter fall a simple mass balance

carbon-allocation-respiration model has been included (Williams et al., 2005; Sus et al., 2010).

Integrating observations and site-specific model at the ecosystem scale allows to investigate the relative sensitivity of interacting processes to changes in evaporative demand/temperature and precipitation. Here we applied a novel combination of field experiment, ecosystem observations and site calibrated soil-plant-atmosphere model. Our objectives were to evaluate the model's ability to capture responses to seasonal drought and reduced soil drought (watering experiment) for a semi-arid regenerating ponderosa pine forest, to determine the sensitivity of carbon and water dynamics to changes in soil and atmospheric drought and to make predictions for scenarios that represent increased drought in the future. Associated with these objectives the following hypotheses were tested: (1) gross primary productivity is more susceptible to changes in atmospheric demand than to changes in summer precipitation, (2) photosynthesis will be more sensitive than heterotrophic respiration to changes in water availability and temperature, and (3) increasing summer drought severity will be compensated by lengthening of the growing season.

2   Methods

2.1   Study site

The study site (US-Me6) is located east of the Cascade mountains in Central Oregon (977 m a.s.l., 44°19′25.5″N, −121°36′18.4″E) and is part of the Metolius cluster sites within the AmeriFlux network. After a wildfire in 1979 the site was salvage logged, became US Forest Service land and has been re-forested with ponderosa pine trees in 1986 to supplement natural regeneration. Due to poor survival additional inplanting was conducted in 1990. The dominant overstory vegetation is 22 to 26 yr old *Pinus ponderosa* with an average height of 5.2 ± 1.1 m and summer maximum overstory half-sided leaf area index (LAI) of $0.8\,m^2\,m^{-2}$ in 2010. Tree density is low with 162

trees ha^{-1}. The understory vegetation is scattered and dominated by antelope bitterbrush (*Purshia tridentata* (Pursh) D.C.) and grasses (predominantly *Bromus tectorum* L.), estimated to account for a LAI of 0.1 m^2 m^{-2}. The soil is a freely draining sandy loam (82 % sand, 16 % silt, 2 % clay), derived from volcanic ash (soil depth > 1.2 m).

5 The climate can be characterized as Mediterranean with hot, dry summers and cool, wet springs and winters. The long-term 30 yr (1971–2000) precipitation average for the study site is 460 mm with large inter-annual variability. Averaged minimum and maximum monthly temperatures range between –5.5 and 10.5 °C in winter and between 2.5 and 27.8 °C in summer (PRISM Climate Group, Oregon State University,

10 http://prism.oregonstate.edu, created 31 October 2008).

2.2 Observational data

A variety of ecosystem measurements were carried out, including net ecosystem exchange of carbon dioxide (CO_2) and water (H_2O) using the eddy covariance approach, tree transpiration derived from sap flow estimates, soil and heterotrophic respiration,

15 biomass inventories, leaf area index and phenological observations in 2010 and 2011. To test the effects of water availability we conducted a two yr watering experiment during the summer drought season and compared responses of watered trees and soil to control plots ($n = 5$ trees per treatment). A detailed description of the experimental set up, measurements and data processing, including gap-filling of eddy covari-

20 ance data and analysis can be found in Ruehr et al. (2012). All further measurements conducted for model parameterization and validation are briefly described here. Predawn and midday needle water potentials were measured with a pressure bomb on south-facing fascicles of 5 trees per treatment between June and September 2011. Leaf specific conductance (K_{leaf}) was calculated from pre-dawn and midday leaf wa-

25 ter potential and sap flow measurements (11–13 h) following Irvine et al. (2004). Estimates of photosynthetic capacity (V_{cmax} and J_{max}) were derived from A/Ci curves using a Li-6400 equipped with a Li-6400-02B LED light source (Li-Cor, Lincoln, NB,

USA) on south-facing fascicles. Leaf temperature was set to 25 °C, photosynthetic radiation to $1600 \, \mu mol \, m^{-2} \, s^{-1}$ and water vapor concentrations were close to ambient conditions. The CO_2 concentrations used to generate the A/Ci curves were 390, 200, 100, 40, 390, 500, 700, 850, 1200, 1600 ppm. A/Ci data was submitted to Leafweb (http://leafweb.ornl.gov/Pages/LeafWeb.aspx) where V_{cmax} and J_{max} were calculated by a standardized procedure (Gu et al., 2010). Dry weight of root biomass was assessed by sequential coring to 30 cm soil depth in June, August and September, sorted in fine (< 2 mm) and dead roots. Maximum rooting depth was estimated at 1.2 m after excavation of a soil pit, with 50 % of the fine root mass in the 0–30 cm layer, and 50 % distributed over the remainder of the depth.

We derived observational errors from standard deviations between plots and/or measurement campaigns if available (see Tables 1 and 2). The error of annual NEE from eddy covariance was estimated at ±16 % at a young pine site close-by (Vickers et al., 2012). Since NEE fluxes can be positive or negative, defining errors by a coefficient of variation is unsuitable, so instead the error of daily NEE was set at $\pm 0.5 \, g \, C \, m^{-2} \, d^{-1}$. Error estimates for evapotranspiration (ET_{obs}), gross primary productivity (GPP_{obs}), ecosystem respiration ($Reco_{obs}$) and heterotrophic respiration (Rh_{obs}) were set at ±20 %. The error estimate for transpiration (T_{obs}) was set at ±30 %, calculated from standard error of sap flow between trees and the error of stand-scaled sapwood calculation. The error for soil water content (SWC) was set at $\pm 0.2 \, m^3 \, m^{-3}$ as given by the manufacturer (10HS, Decagon Devices, Inc., WA, USA).

To estimate the amount of irrigation water taken up by the watered trees we labeled the irrigation water with deuterium. This increased the isotope ratio of $\delta^2 H$ in the water from −98 ‰ to +103 ‰ ($\delta^2 H$ of water taken up by control trees was −114 ± 4 ‰). For isotope analysis of tree source water we took branch samples on three occasions during the summer 2011, before (17 June) and during the watering treatment (4 August and 22 August) on control and watered trees. Woody branch segments were cut from the trees (> 15 cm away from transpiring needles) and immediately transferred to glass vials with polyseal cone inserts and sealed to prevent evaporation. After cryo-

genic vacuum distillation the water extract was analyzed for isotopic composition by isotope spectrometry (DeltaPlus; Finnigan MAT GmbH, Bremen, Germany) interfaced with a temperature conversion/elemental analyzer (TC/EA; Finnigan MAT). The relative amount of tree water that originates from the irrigation was calculate using a simple mixing model: $f1 = (\delta sample - \delta source_2)/(\delta source_1 - \delta source_2)$. The $\delta^2 H$ values are expressed relative to Vienna Standard Mean Ocean Water.

2.3 The model

The soil-plant-atmosphere model (SPA), is a process based model that simulates ecosystem carbon and water balance processes at fine temporal (30 min) and spatial scales (up to 10 canopy and 20 soil layers). The carbon and water cycle in the model is directly coupled with stomatal conductance set to maximize C gain under limitation of canopy water storage and soil to canopy water transport. To allow for estimates of respiration, C pool dynamics and total net ecosystem exchange, the model has been modified with a simple allocation-respiration model (Williams et al., 2005; Sus et al., 2010). The allocation-respiration model (described in detail by Williams et al., 2005) disaggregates gross primary productivity (GPP) into plant respiration and carbon allocation to leaves, fine roots and woody matter assuming fixed allocations. Turnover rates determine the litter fall from leaves and fine roots to the litter pool (fast turnover organic matter) and from woody matter to the soil organic matter pool (SOM; slow turnover). Litter can become part of the SOM pool depending on turnover and mineralization rates. Heterotrophic respiration (Rh) depends on the size of the litter and SOM pools, mineralization rates, temperature and in our modified version a dependency on soil water content (see below). Autotrophic respiration (Ra) depends on the size of the plant respiratory C pool, the turnover time of this pool and temperature (see below).

In the present study we used SPA v.2.4 (https://www.wiki.ed.ac.uk/display/cesdwiki/SPA) with several adaptations. To improve estimates of soil water potential (SWP), we derived an empirical relationship between SWC and SWP from measurements in 2011 (Fig. S1), as changes in soil water potentials in the porous soils (e.g., Williams

et al., 2001) are only inadequately described by the algorithms normally applied in the model. Our preliminary model testing suggested the ratio of evaporation to transpiration was too low. So we reduced the roughness layer to 10 cm in this very open forest stand and by assuming the soil tortuosity factor of gas diffusion is close to one in porous soils (following Moldrup et al., 2001), we were able to increase evaporation estimates by 39 % in 2010 and 2011, improving simulated ET slightly (reduced RMSE by 3 %). To increase the drought sensitivity in SPA, we added a Weibull function of tree conductance to changes in SWP (Fig. S3), allowing the model to capture the strong drought response of tree transpiration in July and August (see Ruehr et al., 2012).

Concerning the seasonality of carbon fluxes, model testing showed that NEE and GPP were largely overestimated by SPA during winter months and generally had a much reduced seasonality when compared to observations. The reason may be the lack of seasonality of leaf nitrogen and/or photosynthetic capacity in the model. For example, Misson et al. (2006) found that photosynthetic capacity of ponderosa pine shows pronounced seasonality with summer rates of V_{cmax} and J_{max} roughly doubling winter rates measured at the same temperature and light conditions. By adding a factor for daylength control (df) to photosynthetic capacity (V_{cmax} and J_{max} with 25 °C temperature optimum), as found in the CLM4 Community Land Model (df = daylength^2/$_{max}$daylength^2), the agreement between simulated and observed daily GPP, Reco and NEE was substantially improved (reduction of RMSE from 0.71–1.06 to 0.50–0.73 g C m^{-2} day^{-1}). Further adaptions were made to the carbon allocation part of SPA. We included a simple exponential temperature function to turnover of the plant respiratory pool (Ra). For Rh we added a SWC dependency in the form of a sigmoid function to the exponential temperature relationship of mineralization (Fig. S2).

Because conifer phenology in SPA v.2.4 was practically non-existent (constant C allocation to growth), yet ponderosa pine shows distinct seasonality of needle growth, we incorporated a relatively simple phenological term derived from two years of observations of pine phenology. Roughly, we observed bud break by mid of June with most of leaf elongation in July continuing until mid/end of August. The peak of needle fall of

4–5 yr old needles occurred by the end of September. The phenology of the deciduous understory shrubs was slightly out of phase. Bud break was up to one month earlier and the shrubs were largely without leaves by the end of October. However, for simplification we did not explicitly include the deciduous phenology. To implement the pine phenology in the model, we added a growing degree function starting at 1 February with a 5°C threshold (Hannerz, 1999). The growing degree sum was set to 140 after parameterizing to the observed start of bud extension. We used bud extension as the starting point of C allocation to the needles over bud break (about 10 days later), to represent growth of new plant tissue during bud elongation. After the onset of bud extension (unfolding of buds, but needle tips not green yet), C allocation to needle growth was activated and ended after 60 days or by 31 August at the latest (we observed that 90 % of needle elongation was completed by mid August, about 2 months after bud break). In sync with the end of C allocation to needles, needle turnover (about 6 % needle loss in 30 days) was activated to reduce seasonal needle peak by one-quarter of the initial leaf biomass in spring (i.e., 5 yr old needles). The thereby derived seasonal course of leaf biomass translated to an LAI increase of $0.2\,\mathrm{m^2\,m^{-2}}$ during the growing season, with an annual increase in LAI of $0.1\,\mathrm{m^2\,m^{-2}}$, which is well within the range of the observed LAI gain of $0.08\,\mathrm{m^2\,m^{-2}}$ between 2010 and 2011.

2.3.1 Simulation and parameterization

The model was run using half-hourly meteorological data (including temperature, $[CO_2]$, windspeed, shortwave radiation, vapor pressure deficit, photosynthetic active radiation and precipitation) for 3 yr (2009–2011), where 2009 was used as spin-up-run for soil water content and soil temperature. We divided the canopy in 5 layers of equal height with varying leaf biomass. For simplification all layers including the understory were treated as ponderosa pine. Leaf nitrogen content was split equally among the layers, as we did not assume nitrogen to vary substantially with height in the open canopy. For the soil, we assigned 20 soil layers up to 2 m depth, each layer 10 cm thick with constant soil texture.

Most of the data needed for model parameterization were available from measurements (see Tables 1 and 2). Some parameter estimates were derived from Williams et al. (2005) who used data assimilation to parameterize carbon allocation in SPA. These parameters were adjusted in an iterative technique to produce the best agreement with observations (defined by minimum RMSE and highest R^2 between simulated and measured values). First, parameters of the SPA core model were calibrated. Estimates of stem conductivity and root resistivity were derived from leaf specific conductance measures (K_{leaf}, see above). We used these data as the starting point to calibrate simulations with measured daily SWC and tree transpiration. We allowed the model to overestimate tree transpiration to account for transpiration of understory herbs and shrubs (LAI of about $0.1\,\mathrm{m^2\,m^{-2}}$). Allocation of C to leaf growth was the next parameter adjusted to produce leaf biomass close to measured LAI by the end of summer. The allocation to fine root growth was calibrated in two ways, by checking the drought sensitivity of simulated transpiration, and by ensuring that wood growth over the two years equaled stem area increment estimates from dendrometer bands (11 % observed vs. 12 % modeled wood increment in 2011), resulting in an average annual increase in fine root biomass of 10 %. Next, the mineralization rate of SOM and the turnover rate of litter to SOM was tuned to improve estimates of Rh during the two growing seasons. Then, we calibrated the parameters that determine the fraction of GPP respired and the turnover rate of the Ra pool to improve the match of simulated and observed NEE and Reco. Finally, we re-checked the fit of the simulations with the observations and if necessary repeated the calibration steps once more. Data processing and statistical analyses were performed using R 2.11.1 (R Development Core Team, 2010).

The error of simulated daily GPP and NEE due to parameter uncertainty is estimated to range between ±10 % and ±20 % (Williams et al., 2001, 2005). For a detailed sensitivity analysis of the key parameters in SPA, see Williams et al. (2001).

Full Screen / Esc

Printer-friendly Version

Interactive Discussion

2.3.2 Climate scenarios

Future climate for the Pacific Northwest was implemented from the A1B greenhouse gas emission scenario, derived from a suite of models by reliability ensemble averaging (Centre for Science in the Earth System, University of Washington; 2008 scenarios:
http://cses.washington.edu/cig/fpt/ccscenarios.shtml). In general, all seasons are expected to be warmer with the largest temperature increase predicted during summer. Modest changes in precipitation are expected, although changes in precipitation are less certain than changes in temperature. Small increases in precipitation are likely to occur during winter (approx. +4 % in 2040 and +8 % in 2080), while slight precipitation decreases are expected during summer (approx. −12 % in 2040 and −16 % in 2080).

To test the sensitivity of the young pine stand to changes in forcing, simulations were run over 10 yr starting from the same initial conditions with different climate imposed. The 10 yr long data series of future temperature, vapor pressure deficit (VPD) and precipitation were created by iterating the years 2010 and 2011 and adding the expected temperature increase and −10 % and −20 % percent changes in summer precipitation (2010 and 2011 were relatively average years and well within the 1971–2000 temperature and precipitation range derived from PRISM Climate Group, http://prism.oregonstate.edu). Meteorological data from 2009 was changed accordingly and used in the spin-up-run. Because extreme events are likely to increase, rain amounts were experimentally reduced by 50 % and 100 % between June and August and simulations run accordingly. We tested the sensitivity to the following scenarios: (a) reduced summer precipitation, (b–c) increased summer temperatures (2040 and 2080) in combination with reductions in summer precipitation and (d–e) warming across all seasons (2040 and 2080) in combination with reductions in summer precipitation. Because long-term stimulating effects of CO_2 are highly uncertain and likely limited by nitrogen for which SPA does not account for, all future climate scenarios were implemented under current atmospheric CO_2 concentrations of 390 ppm (see Discussion).

Heat and drought impacts on semi-arid forest

N. K. Ruehr et al.

Title Page

Abstract	Introduction
Conclusions	References
Tables	Figures

|◄ | ►|

◄ | ►

Back | Close

Full Screen / Esc

Printer-friendly Version

Interactive Discussion

3 Results

3.1 Model performance and drought response

The two study years 2010 and 2011 showed a distinct seasonality, with coldest temperatures during winter dropping as low as $-25\,°C$, and maximum temperatures up to $34\,°C$ during the mainly dry summer months July and August (Fig. 1). Similarly, ecosystem water and CO_2 exchange was lowest during winter and peaked in June/July at the beginning of the dry season (Figs. 1 and 2). Seasonal flux dynamics were generally well captured by SPA, and the performance of the model to predict observations from the meteorological data is confirmed by linear regressions between simulated and observed daily fluxes ($R^2 = 0.63 - 0.87$; Fig 3).

Comparing simulated (sim) and observed (obs) NEE dynamics in more detail (Fig. 2a–b), we found good agreement with the seasonal course, however, fluxes at the lower and higher range diverged from the one-to-one line (Fig 3f). Simulated GPP and Reco were compared to the observations (derived from NEE partitioning) and showed that simulation overestimated fluxes during early spring and annually by 12 and 20 %, respectively (Figs. 2c–d, 1e–j and Table 3). However, the annual estimates of NEE agreed very well with only $21\,g\,C\,m^{-2}\,yr^{-1}$ or less than 10 % difference between simulated and observed values in 2011 (Table 3). Thus, the calibrated model is capable of producing daily estimates of NEE, GPP and Reco largely within the uncertainties of the observations.

Discrepancies between simulated and observed ET were 24 % in 2010 and 18 % in 2011, but still close to the uncertainty estimates of the observations (±20 %). Large differences were found during summer, where ET_{sim} was smaller than ET_{obs} by an average of 43 % (88 mm) in 2010 and 31 % (66 mm) in 2011 (Fig. 3c). The underestimation of ET_{sim} might partly originate from a slight underestimation of observed SWC above $0.1\,m^3\,m^{-3}$ (Figs. 1c–d and 3a). Although ET_{sim} was underestimated, simulated daily transpiration (T_{sim}) followed closely the dynamics in observed tree transpiration

(T_obs) derived from tree sap flow measurements (Fig. 3d). Because understory shrubs account for approximately 15 % of LAI and we did not have transpiration measurements for shrubs, we intentionally allowed T_sim to be higher to account for understory transpiration and to improve the fit with the whole ecosystem ET observations.

Next, we focus on the largely rain-free, summer drought season that extended from about mid June to mid/end September in both study years. The precipitation regime in summer was different for the two years. In 2010 small rain events began in early September, but in 2011, the drought was interrupted by cool and moist weather and an unusual large rain event of 23 mm in mid July, followed by a dry period without rain through the end of September. Despite these different patterns in precipitation variability, the amount of rain from June to August was similar with 52 mm and 53 mm, and SWC (0–40 cm) was as low as 0.05 $\text{m}^3 \text{m}^{-3}$ by September during both years (Fig. 1c–d). Both summer seasons were characterized by a strong reduction of all fluxes by the end of August (Figs. 1 and 2), following largely the course of increasing soil and atmospheric drought. These patterns were also displayed in the simulation, with all fluxes decreasing in response to the seasonal drought. The relationship of modeled and observed values during the dry season is largely confirmed by the linear dependencies, close to the one-one line (see Fig 3). The unusual rain event in July 2011 allowed us to test the performance of SPA to instantaneous changes in water availability. ET_sim and T_sim matched the observations closely: at first, both fluxes increased strongly in response to the rain event, followed by an immediate decline along with increasing VPD. Respiratory fluxes followed a similar response but declined steadily with reductions in SWC (Fig. 2c–f). Application of the sigmoid SWC function (Fig. S2) in the temperature dependency of mineralization resulted in a drought response of Rh_sim that closely matched the observed daily values (± 18 %) and was within the error estimate of Rh_obs (Figs. 2e–f and 3h).

Summarizing, despite some discrepancies between simulated and observed ET during summer, we can highlight that the modified soil-plant-atmosphere model (SPA v2.4)

Full Screen / Esc

Printer-friendly Version

Interactive Discussion

performed well in capturing the seasonality as well as drought response of water and carbon fluxes in the regenerating semi-arid pine forest.

3.2 Effects of increased soil water availability

The sensitivity of SPA to changes in water availability was tested by increasing the amount of summer precipitation step-wise to equal water supplied to the irrigation treatment in summer 2010 and 2011. This allowed us to study the effects of water availability apart from atmospheric drought on the C balance of the pine forest. Focusing on the simulation run with water additions equaling the irrigation treatment (i.e., 100 %, see Fig. 4), we found pronounced discrepancies in soil water content and fluxes between simulation and observation. SWC and T were on average about 35 % and 120 % overestimated in the simulation. In addition, SWC_{obs} decreased immediately after the end of watering (Fig. 4a–b, the gray area marks the duration of the irrigation period), while SWC_{sim} stayed relatively high. The reason for these differences may be in the relatively small area watered ($4\,m^2$ around each tree) causing higher soil evaporation than assumed in the model (compared to no water additions soil temperatures were 2 °C lower in the simulation but only 0.7 °C lower in the observation). Moreover, we can not exclude the possibility that some of the added water may have been taken up by shrubs and trees close-by and that the measured trees were partially rooting outside the watered area. This makes comparing the experimental with the modeling results challenging.

However, a good agreement of the field experiment (+436 mm in 2010 and +582 mm in 2011) and model was found for T and Rh when simulated water additions were as low as 174 mm (i.e., the 40 % scenario in 2010 and 30 % in 2011, Fig. 4c–d and i–j). Interestingly, this is confirmed by the relative amount of irrigation water taken up by the trees in the experiment. Isotope analysis of δH^2 in tree source water showed that the percentage of water taken up by trees that was from the irrigation was 21±7 % on 4 August and 20±3 % on 22 August 2011. This result agrees with the cumulative increase in T_{obs} (+23 %) which compares well with the cumulative increase of T_{sim} (+29 %) during

Heat and drought impacts on semi-arid forest

N. K. Ruehr et al.

Title Page

Abstract	Introduction
Conclusions	References
Tables	Figures

|◀ | ▶|

◀ | ▶

Back | Close

Full Screen / Esc

Printer-friendly Version

Interactive Discussion

the watering period in 2011. Thus, the good accordance in tree water uptake and T of the 30 % scenario (+174 mm) with the observations (+582 mm) suggests that the extra water available for the trees must have been much less in the field experiment than the simulation of the 100 % scenario implied. Effects on soil water potential (SWP) in re-
5 sponse to the watering further confirmed this. The increase of SWP in response to field water additions (+0.2 MPa) compared well to that under the 30 % scenario (+0.3 MPa, compare to +0.5 MPa under the 100 % scenario; see Fig. S4).

Considering the overall effects of summer water additions on simulated annual C fluxes, a small but clear negative effect on annual NEE_{sim} was found for water additions
10 below 200 mm (Table 4), in agreement with the experimental results (when > 400 mm of water was added; Ruehr et al., 2012). This negative effect of water additions on NEE results from a larger increase in heterotrophic respiration than photosynthesis.

3.3 Climate scenarios

To evaluate the effects of intensifying droughts and warmer temperatures on the carbon
15 and water balance of the young pine plantation, we ran SPA over a 10 yr period starting from the same initial conditions but with different climate imposed (CO_2 concentrations remained at 2010/2011 conditions). Percent responses were calculated from averaged annual changes relative to the 2010/11 control conditions.

Summer rain (June–August) was reduced without changing its variability, stepwise
20 by 10, 20, 50 and 100 % (i.e., 100 % reduction is about −52 mm or −12 % annually; resulting in summer SWC reduction of 20 %). These reductions in summer rain are similar to the dry years in the early 2000s with precipitation anomalies of −31 % to −85 % during summer (compared to the average summer precipitation of 43 mm be-tween 1971–2010; PRISM Climate Group). As expected, no rain caused the strongest
25 decline in all fluxes with 9 % to 12 %, but the decrease was not linear (Fig. 5a). The response of NEE to 50 % summer rain reduction (−10 %) was nearly as large as under 100 % rain reduction (−12 %), which only caused NEE to decrease by an additional

2 %. The response of Rh and GPP followed similar patterns, but the relative decline in Rh was slightly less than that of GPP.

Increased summer heat of up to 38.5 °C had a pronounced negative effect on simulated annual fluxes (Fig. 5b–c), biomass and soil organic matter (Fig. 6b–c). This was contrasted by Rh being relatively unaffected, causing NEE to decline sharply. An increase in summer temperatures of +3 °C and +4.5 °C, along with a 30 % and 40 % increase in VPD, led to a −24 % and −38 % reduction in NEE (Fig. 5b–c). SPA did not predict pronounced interactive heat and drought effects. For example, in response to 2080 summer temperatures and 100 % rain reduction, the simulated 51 % decline in NEE was almost additive (+4.5 °C: −40 % and −100 % rain: −12 %). This is in contrast to most multifactorial experiments which show additive effects to be rare (Dieleman et al., 2012). However, it can be speculated that with increasing length of the model runs (i.e., from 2010–2080) SPA would allow for further accumulation and feedback of the responses.

The negative effects of hotter summers were largely offset by the warmer winter/ spring conditions under the full 2040 and 2080 temperature scenarios at current [CO_2] (Fig. 5d–e). Rh increased in response to the warming (2040: +5 % and 2080 +8 %; Fig. 5d–e), reducing soil organic matter (2040: −1.7 % and 2080: −2.1 %; Fig. 6d–e). GPP and T also increased slightly, while the C sink remained weaker compared to the 2010/11 reference. The relative effects on biomass varied. Needle biomass increased, while root and woody biomass declined. Taking a closer look on the seasonal course of differences in averaged cumulative fluxes reveals interesting patterns (Fig. 7). Cumulative GPP and NEE were much larger during the first half of the year under the 2040 and 2080 scenarios compared to the 2010/11 baseline (Fig. 7a–b, solid lines). The warmer winter/spring temperatures improved the conditions for photosynthesis and also caused bud elongation to occur earlier (5 May in 2080 vs. 6 June in 2010/11). This increased the length of the favorable growing conditions before the start of the drought season. In accordance, the model predicted cumulative GPP to be 100 g C m^{-2} and NEE to be about 40 g C m^{-2} on average larger by June in 2080, followed by a sharp

decline during the summer dry season (Fig. 7a–b). Interestingly, annual NEE remained below the 2010/11 reference despite an increase in needle biomass (Fig. 6d–e). Larger needle biomass was accompanied by a small decrease in root and woody biomass, which caused the needle to root ratio to increase (Fig. 6d–e). An imbalance in the ratio of above- to belowground biomass could lead to an increase in drought stress over the long-term, with a possible threshold at which ponderosa pine may not survive.

4   Discussion

4.1   Model evaluation

Our modified and calibrated version of the SPA model did successfully simulate the observed seasonality and drought response of a semi-arid ponderosa pine forest. Simulated NEE was within the uncertainty estimates of observed NEE in 2011. Also simulated annual ET estimates were within the error of the observations, but with pronounced seasonal discrepancies. Larger differences between simulated and measured ET during summer have been found in other pine forests using SPA (Schwarz et al., 2004). Since we found transpiration to be rather overestimated by the model, the differences in simulated and observed ET are likely caused by underestimation of soil evaporation. A possible explanation might be an overestimation of shallow root density that decreases water partitioning towards evaporation. Moreover, in very open forest stands, due to large gaps in canopy cover, net radiation transmitted to the forest floor can be larger than a multi-layer canopy model with equal leaf distribution implies, resulting in an underestimation of soil evaporation (Law et al., 2001). Our study site has a open canopy with low tree density and the overstory leaf area index ranges locally from 0 to $2\,\mathrm{m^2\,m^{-2}}$. This results in a large fraction of the soil to receive direct radiation, not accounted for in the modeling and in addition causes large variability in root distribution. Thus, including the heterogeneous nature of open forest stands in canopy

cover and horizontal root distribution, may improve evaporation predictions especially in Mediterranean and semi-arid regions.

Considering drought effects, we found SPA to perform well in predicting the decline of measured component fluxes. The earlier and stronger reduction in GPP than Reco during drought stress, which causes NEE to decline relatively more (Schwalm et al., 2009; Ruehr et al., 2012), was captured by the modified model. Generally, during drought the ratio of respiration to photosynthesis may increase (Flexas et al., 2006). Measurements of night-time needle respiration in ponderosa pine showed a 50 % decrease in respiration compared to a 80 % reduction in net photosynthesis by early September 2011 (data not shown). In agreement, SPA was able to predict Ra to reduce less than GPP in response to the drought (compare 40 % reduction of Ra to 60 % reduction of GPP by September 2011). This supports our relatively simple way of modeling Ra from constant C allocation to the Ra pool with monthly turnover and a temperature-dependency of respiration.

Interpreting the mismatch between observed and modeled ecosystem responses to the experimental water additions is challenging, due to a multitude of factors involved. However, we think that the disagreement between model and experiment is not caused by the model's failure in capturing plant physiological processes, but rather by a larger amount of water available to the vegetation in the simulation than under field conditions, due to experimental design and trees rooting outside the watered area. This is suggested by the larger soil water content in the simulation than under experimental field conditions, and by the good agreement in soil water potential, water uptake and transpiration between experiment and model under reduced water additions. In addition, this confirms the water sensitivity of the model's hydraulic pathway during summer conditions. Interestingly, with water additions of < 200 mm the model confirms the overall experimental result. Increased water availability (while atmospheric conditions are unchanged) can result in a reduction of NEE due to a larger increase in Rh than photosynthesis (see Ruehr et al., 2012). This clearly demonstrates that the SPA model

was able to predict the experimental result of decomposition being tightly soil moisture limited during summer drought conditions.

4.2 Temperature vs. precipitation effects

The severity of droughts depends on both the amount of water available and temperature affecting atmospheric water deficit. Ranking their relative control on plant physiological processes is challenging as summer droughts are generally characterized by declining soil water content and a temperature dominated increase in atmospheric vapor pressure deficit (De Boeck and Verbeeck, 2011). Watering trees during seasonal summer drought provided us with the opportunity to study the effects of atmospheric drought apart from soil water limitation. The overall weak response of pine physiology to increased soil water in the field experiment point to a strong limitation of VPD (and thus temperature) on plant gas exchange (Ruehr et al., 2012). This was largely confirmed by the model. For example, a tripling of summer precipitation (causing a 40 % increase in SWC) under drought-typical VPD conditions, increased GPP only by +5 % in 2010 and +8 % in 2011. Indeed, stomatal conductance in young ponderosa pine is found to be tightly regulated when atmospheric water demand is large even under non-limiting soil water conditions (Ruehr et al., 2012). A threshold for minimum stomatal conductance was found at VPD of about 3.5 kPa, relatively independent of soil water content. This isohydric behavior of stomatal control has often been observed in pines (Martinez-Vilalta et al., 2004; Maseyk et al., 2008). Stomata close to maintain midday leaf water potentials relatively constant regardless of soil water availability (McDowell et al., 2008).

The tight regulation of tree water loss explains the strong decline of photosynthesis with increasing summer temperatures. Temperature has been confirmed to be an important driver of drought stress in US forests by exponentially increasing evaporative demand (Williams et al., 2013). In our study, summer temperatures as predicted for 2080 (+4.5 °C) caused a 40 % increase in VPD that resulted in 17 % decline in GPP and a 19 % reduction in leaf biomass compared to the 2010/11 simulation. Interest-

Heat and drought impacts on semi-arid forest

N. K. Ruehr et al.

Title Page

Abstract | Introduction

Conclusions | References

Tables | Figures

◄ | ►

◄ | ►

Back | Close

Full Screen / Esc

Printer-friendly Version

Interactive Discussion

ingly, extreme temperatures during summer drought affected the forest water balance by slightly enhancing evaporation (+3%), but decreasing transpiration (due to tight stomata control and reduced biomass). However, we found the net effect on soil water content to be minimal (< 1%). Thus, increased vapor pressure deficit causing stomata closure was the explanatory factor reducing GPP and biomass. In summary, these findings confirm our first hypothesis that GPP in isohydric pine is affected more by changes in atmospheric demand than summer precipitation.

The strong reduction in GPP was opposed by minimal effects on Rh in response to hotter summer temperatures (Table 5), because temperature increases did compensate for reductions in litter input and soil organic matter (see next section below). The net effect was that NEE declined relatively more (−38%) causing a larger reduction in the ecosystem's C sink strength under hotter than drier summer conditions.

4.3 Effects of warmer and drier climate

We concentrated our study on summer drought effects and temperature increases and did not account for elevated atmospheric CO_2 in the simulation runs. Short-term effects of increased CO_2 include stimulation of photosynthesis and reduced transpiration rates, while long-term effects can lead to acclimation processes and nitrogen limitation, causing down regulation of photosynthetic activity and production (see review by Smith and Dukes, 2013). This down-regulation and decreased CO_2 response has been shown to be stronger in low compared to high nutrient systems (Ainsworth and Long, 2005). Thus, we can not exclude positive effects of elevated CO_2 on GPP, but we may expect these responses to be relatively small in the nutrient-poor ponderosa pine systems in Central Oregon.

Increases in summer heat and drought severity reduced simulated NEE by 24 to 51% compared to the 2010/11 reference. This agrees with the effect of the turn of century drought (2000–2004) that led on average to a 37% reduction in NEE of evergreen needleleaf forests in western North America (Schwalm et al., 2012). The strong reduction in NEE was caused by a larger decline in GPP than heterotrophic respira-

Back | Close

Full Screen / Esc

Printer-friendly Version

Interactive Discussion

tion (Table 5). This pattern is commonly found by ecosystem studies and models (e.g., Shi et al., 2013, this special issue), and can be largely explained by two processes that may act in concert. First, increasing temperatures during drought periods may cause additional restrictions on GPP (see detailed explanation above), but may partially compensate for soil moisture constrains on decomposition (Irvine et al., 2008; Ruehr et al., 2012). Second, large soil C pools and litter inputs downstream of GPP may buffer and lag responses of decomposition. This indicates that initially pronounced differences in Rh and GPP could diminish if soil C pools decline under continuing soil drought (Shi et al., 2013). Interestingly, we found contrasting responses of decomposition rates and soil carbon pools in response to hotter summer temperatures. Large declines in GPP reduced litter production and soil organic matter decreased, but Rh was apparently relatively unaffected. A possible explanation is that increased temperatures largely compensated for reducing soil carbon pools by stimulating decomposition. However, one may speculate that the temperature-induced facilitation of decomposition dampens over the long-term along with reductions in soil C pools, causing the relative difference in the responses of Rh and GPP to decline with time.

Considering warming trends across all seasons, the complexity of ecosystem responses increased (Table 5). The negative effect of increasing drought severity was largely balanced by positive effects on early season GPP, due to more favorable winter and spring conditions. However, this was contrasted by stimulations of Rh and adverse changes in above- and belowground biomass, triggered by earlier bud break.

Bud break was predicted to occur up to one month earlier in 2080, causing a shift in the needle growth phenophase mainly towards the more favorable growing conditions before the seasonal summer drought. Needle growth in pine has been described to occur largely in summer (Maseyk et al., 2008), supported by photosynthates gained during the growing season (Klein et al., 2005). In agreement, needle growth in SPA directly depends on recent assimilates. Thus, needle biomass in the model increased due to C allocation to needle growth starting earlier. This also affected the amount of needle litter available by late summer which stimulated heterotrophic respiration. More-

Heat and drought impacts on semi-arid forest

N. K. Ruehr et al.

over, increases in needle production affected allocation patterns causing an increase in the ratio of needle to root and woody biomass. This is partly contradictory to a meta-analysis on the ratio of leaf to sapwood area in pines, where trees grown under larger atmospheric water deficit showed a reduction in the ratio of leaf biomass to stem area
5 (DeLucia et al., 2000). In agreement with this study, SPA predicted increasing summer heat and drought to reduce needle biomass more than root and woody biomass. Positive effects on needle production only occurred in response to winter and spring warming. We can not further verify our findings, as to our knowledge there are no studies on the combined effects of warmer winter/spring temperatures and increased
10 summer drought on pine phenology and C allocation patterns. Thus, one could argue these changes in biomass to be an artifact of the relatively simple allocation and phenology model we used. However, since needle growth depends largely on current photosynthates and fine root growth in ponderosa pine shows a single peak of production at the end of May (Andersen et al., 2008), one could also speculate that an earlier
15 onset of needle growth may lead to a competition scenario between newly developing roots and needles. Such an shift of intensified demand for current photosynthates may become a relevant threshold component for the pine's survival of drought stress over the long-term.

In summary, the model results largely confirm our third hypothesis that the earlier
20 start of the growing season may compensate the negative effects of more extreme summer droughts. But they also highlight that the long-term net effect may depend on the degree of heterotrophic respiration responding, and on the sensitivity of water and nutrient supply to changes in plant allocation patterns.

5 Conclusions

25 The calibrated soil-plant-atmosphere model was successfully validated against measurements from a regenerating semi-arid pine forest. Testing the model with results from a field watering experiment revealed differences in water availability that may be

largely an artifact of the experimental design (i.e., the small area watered). However, assuming the same increase in tree water availability between model and experiment (derived from isotope measurements of tree source water), a good agreement of simulated and observed flux dynamics was found. The small response of transpiration and photosynthesis to water additions in both the field experiment and modeling clearly showed that heat executes a tight control on ponderosa pine physiology. In agreement, the decline in simulated annual GPP, NEE and biomass was three times larger in response to hotter summer temperatures than reduced precipitation. These negative effects were largely mitigated under the all season warming scenarios because of increased early season GPP and earlier bud break. In turn, this changed allocation patterns causing needle production to increase, while root production declined compared to the 2010/11 reference. The predicted imbalance in above- to belowground biomass may accelerate water stress over the long-term to a threshold at which ponderosa pine may not survive. This highlights that, in order to quantify future effects of increasing drought severity, an integrated understanding of ecosystem processes responding to the combination of trends and extremes is needed.

Supplementary material related to this article is available online at http://www.biogeosciences-discuss.net/11/551/2014/bgd-11-551-2014-supplement.pdf.

Title Page

Abstract | Introduction

Conclusions | References

Tables | Figures

◄ | ►

◄ | ►

Back | Close

Full Screen / Esc

Printer-friendly Version

Interactive Discussion

References

Ainsworth, E. A. and Long, S. P.: What have we learned from 15 years of free-air CO_2 enrichment (FACE)?, A meta-analytic review of the responses of photosynthesis, canopy properties and plant production to rising CO_2, New Phytol., 165, 351–372, doi:10.1111/j.1469-8137.2004.01224.x, 2005. 571

Andersen, C. P., Phillips, D. L., Rygiewicz, P. T., and Storm, M. J.: Fine root growth and mortality in different-aged ponderosa pine stands, Can. J. Forest Res., 38, 1797–1806, doi:10.1139/X08-029, 2008. 573, 581

De Boeck, H. J. and Verbeeck, H.: Drought-associated changes in climate and their relevance for ecosystem experiments and models, Biogeosciences, 8, 1121–1130, doi:10.5194/bg-8-1121-2011, 2011. 570

DeLucia, E., Maherali, H., and Carey, E.: Climate-driven changes in biomass allocation in pines, Glob. Change Biol., 6, 587–593, doi:10.1046/j.1365-2486.2000.00338.x, 2000. 573

Dieleman, W. I. J., Vicca, S., Dijkstra, F. A., Hagedorn, F., Hovenden, M. J., Larsen, K. S., Morgan, J. A., Volder, A., Beier, C., Dukes, J. S., King, J., Leuzinger, S., Linder, S., Luo, Y., Oren, R., de Angelis, P., Tingey, D., Hoosbeek, M. R., and Janssens, I. A.: Simple additive effects are rare: a quantitative review of plant biomass and soil process responses to combined manipulations of CO_2 and temperature, Glob. Change Biol., 18, 2681–2693, doi:10.1111/j.1365-2486.2012.02745.x, 2012. 567

Domec, J., Warren, J., Meinzer, F., Brooks, J., and Coulombe, R.: Native root xylem embolism and stomatal closure in stands of Douglas-fir and ponderosa pine: mitigation by hydraulic redistribution, Oecologia, 141, 7–16, doi:10.1007/s00442-004-1621-4, 2004. 554

Easterling, D. R., Wallis, T. W. R., Lawrimore, J. H., and Heim, Richard, R., J.: Effects of temperature and precipitation trends on US drought, Geophys. Res. Lett., 34, L20709, doi:10.1029/2007GL031541, 2007. 553

Fisher, R. A., Williams, M., Da Costa, A. L., Malhi, Y., Da Costa, R. F., Almeida, S., and Meir, P.: The response of an Eastern Amazonian rain forest to drought stress: results and mod-

Title Page

Abstract | Introduction

Conclusions | References

Tables | Figures

◀ | ▶

Back | Close

Full Screen / Esc

Printer-friendly Version

Interactive Discussion

elling analyses from a throughfall exclusion experiment, Glob. Change Biol., 13, 2361–2378, doi:10.1111/j.1365-2486.2007.01417.x, 2007. 554

Flexas, J., Bota, J., Galmes, J., Medrano, H., and Ribas-Carbó, M.: Keeping a positive carbon balance under adverse conditions: responses of photosynthesis and respiration to water stress, Physiol. Plantarum, 127, 343–352, 2006. 569

Gu, L., Pallardy, S. G., Tu, K., Law, B. E., and Wullschleger, S. D.: Reliable estimation of biochemical parameters from C_3 leaf photosynthesis-intercellular carbon dioxide response curves, Plant Cell Environ., 33, 1852–1874, doi:10.1111/j.1365-3040.2010.02192.x, 2010. 557

Hannerz, M.: Evaluation of temperature models for predicting bud burst in Norway spruce, Can. J. Forest Res., 29, 9–19, 1999. 560, 581

Hanson, P. and Weltzin, J.: Drought disturbance from climate change: response of United States forests, Sci. Total Environ., 262, 205–220, 2000. 554

Hudiburg, T. W., Law, B. E., and Thornton, P. E.: Evaluation and improvement of the Community Land Model (CLM4) in Oregon forests, Biogeosciences, 10, 453–470, doi:10.5194/bg-10-453-2013, 2013. 554

Irvine, J., Law, B., Kurpius, M., Anthoni, P., Moore, D., and Schwarz, P.: Age-related changes in ecosystem structure and function and effects on water and carbon exchange in ponderosa pine, Tree Physiol., 24, 753–763, 2004. 554, 556

Irvine, J., Law, B. E., Martin, J. G., and Vickers, D.: Interannual variation in soil CO_2 efflux and the response of root respiration to climate and canopy gas exchange in mature ponderosa pine, Glob. Change Biol., 14, 2848–2859, 2008. 572

Kelliher, F., Ross, D., Law, B., Baldocchi, D., and Rodda, N.: Limitations to carbon mineralization in litter and mineral soil of young and old ponderosa pine forests, Forest Ecol. Manag., 191, 201–213, 2004. 581

Klein, T., Hemming, D., Lin, T., Grunzweig, J., Maseyk, K., Rotenberg, E., and Yakir, D.: Association between tree-ring and needle δC_{13} and leaf gas exchange in *Pinus halepensis* under semi-arid conditions, Oecologia, 144, 45–54, doi:10.1007/s00442-005-0002-y, 2005. 572

Law, B., Cescatti, A., and Baldocchi, D.: Leaf area distribution and radiative transfer in open-canopy forests: implications for mass and energy exchange, Tree Physiol., 21, 777–787, 2001. 568

Martinez-Vilalta, J., Sala, A., and Pinol, J.: The hydraulic architecture of Pinaceae – a review, Plant Ecol., 171, 3–13, 2004. 553, 570

Heat and drought impacts on semi-arid forest

N. K. Ruehr et al.

Maseyk, K. S., Lin, T., Rotenberg, E., Gruenzweig, J. M., Schwartz, A., and Yakir, D.: Physiology-phenology interactions in a productive semi-arid pine forest, New Phytol., 178, 603–616, doi:10.1111/j.1469-8137.2008.02391.x, 2008. 570, 572

McDowell, N., Pockman, W. T., Allen, C. D., Breshears, D. D., Cobb, N., Kolb, T., Plaut, J., Sperry, J., West, A., Williams, D. G., and Yepez, E. A.: Mechanisms of plant survival and mortality during drought: why do some plants survive while others succumb to drought?, New Phytol., 178, 719–739, doi:10.1111/j.1469-8137.2008.02436.x, 2008. 553, 554, 570

Misson, L., Tu, K., Boniello, R., and Goldstein, A.: Seasonality of photosynthetic parameters in a multi-specific and vertically complex forest ecosystem in the Sierra Nevada of California, Tree Physiol., 26, 729–741, 2006. 559

Moldrup, P., Olesen, T., Komatsu, T., Schjonning, P., and Rolston, D.: Tortuosity, diffusivity, and permeability in the soil liquid and gaseous phases, Soil Sci. Soc. Am. J., 65, 613–623, 2001. 559

Mote, P., Bethel, J., Capalbo, S., Dalton, M., Eigenbrode, S., Glick, P., Houston, L., Littell, J., Lynn, K., Raymondi, R., Reeder, W., and Snover, A.: Climate Change in the Northwest, Brief Summary„ 2013. 553

Pierce, J., Meyer, G., and Jull, A.: Fire-induced erosion and millennialscale climate change in northern ponderosa pine forests, Nature, 432, 87–90, 2004. 554

R Development Core Team: R: A Language and Environment for Statistical Computing, R Foundation for Statistical Computing, Vienna, Austria, 2010. 561

Ruehr, N. K., Martin, J. G., and Law, B. E.: Effects of water availability on carbon and water exchange in a young ponderosa pine forest: above- and belowground responses, Agr. Forest Meteorol., 164, 136–148, doi:10.1016/j.agrformet.2012.05.015, 2012. 553, 556, 559, 566, 569, 570, 572

Schwalm, C. R., Williams, C., Schaefer, K., Arneth, A., Bonal, D., Buchmann, N., Chen, J., Law, B. E., Lindroth, A., Luyssaert, S., Reichstein, M., and Richardson, A. D.: Assimilation exceeds respiration sensitivity to drought: a FLUXNET synthesis, Glob. Change Biol., 16, 657–670, 2009. 553, 569

Schwalm, C. R., Williams, C. A., Schaefer, K., Baldocchi, D., Black, T. A., Goldstein, A. H., Law, B. E., Oechel, W. C., Paw U, K. T., and Scott, R. L.: Reduction in carbon uptake during turn of the century drought in western North America, Nat. Geosci., 5, 551–556, 2012. 553, 571

Schwarz, P., Law, B., Williams, M., Irvine, J., Kurpius, M., and Moore, D.: Climatic vs. biotic constraints on carbon and water fluxes in seasonally drought-affected ponderosa pine ecosystems, Global Biogeochem. Cy., 18, GB4007, doi:10.1029/2004GB002234, 2004. 568

Shi, Z., Thomey, M. L., Mowll, W., Litvak, M., Brunsell, N. A., Collins, S. L., Pockman, W. T., Smith, M. D., Knapp, A. K., and Luo, Y.: Differential effects of extreme drought on production and respiration: synthesis and modeling analysis, Biogeosciences Discuss., 10, 16043–16074, doi:10.5194/bgd-10-16043-2013, 2013. 572

Smith, N. G., and Dukes, J. S.: Plant respiration and photosynthesis in global-scale models: incorporating acclimation to temperature and CO_2, Glob. Change Biol., 19, 45–63, doi:10.1111/j.1365-2486.2012.02797.x, 2013. 571

Sus, O., Williams, M., Bernhofer, C., Beziat, P., Buchmann, N., Ceschia, E., Doherty, R., Eugster, W., Gruenwald, T., Kutsch, W., Smith, P., and Wattenbach, M.: A linked carbon cycle and crop developmental model: Description and evaluation against measurements of carbon fluxes and carbon stocks at several European agricultural sites, Agr. Ecosyst. Environ., 139, 402–418, doi:10.1016/j.agee.2010.06.012, 2010. 555, 558

Vickers, D., Thomas, C. K., Pettijohn, C., Martin, J. G., and Law, B. E.: Five years of carbon fluxes and inherent water-use efficiency at two semi-arid pine forests with different disturbance histories, Tellus B, 64, 17159, doi:10.3402/tellusb.v64i0.17159, 2012. 557

Williams, A. P., Allen, C. D., Macalady, A. K., Griffin, D., Woodhouse, C. A., Meko, D. M., Swetnam, T. W., Rauscher, S. A., Seager, R., Grissino-Mayer, H. D., Dean, J. S., Cook, E. R., Gangodagamage, C., Cai, M., and McDowell, N. G.: Temperature as a potent driver of regional forest drought stress and tree mortality, Nature Climate Change, 3, 292–297, doi:10.1038/NCLIMATE1693, 2013. 553, 570

Williams, M., Law, B., Anthoni, P., and Unsworth, M.: Use of a simulation model and ecosystem flux data to examine carbon-water interactions in ponderosa pine, Tree Physiol., 21, 287–298, 2001. 554, 558, 561

Williams, M., Schwarz, P., Law, B., Irvine, J., and Kurpius, M.: An improved analysis of forest carbon dynamics using data assimilation, Glob. Change Biol., 11, 89–105, 2005. 555, 558, 561, 581

Williams, M., Rastetter, E., Fernandes, D., Goulden, M., Wofsy, S., Shaver, G., Melillo, J., Munger, J., Fan, S., and Nadelhoffer, K.: Modelling the soil-plant-atmosphere continuum in a Quercus-Acer stand at Harvard forest: The regulation of stomatal conductance

by light, nitrogen and soil/plant hydraulic properties, Plant Cell Environ., 19, 911–927, doi:10.1111/j.1365-3040.1996.tb00456.x, 1996. 554

Wright, J. K., Williams, M., Starr, G., McGee, J., and Mitchell, R. J.: Measured and modelled leaf and stand-scale productivity across a soil moisture gradient and a severe drought, Plant Cell Environ., 36, 467–483, doi:10.1111/j.1365-3040.2012.02590.x, 2013. 553, 554

Zeppel, M., Macinnis-Ng, C., Palmer, A., Taylor, D., Whitley, R., Fuentes, S., Yunusa, I., Williams, M., and Eamus, D.: An analysis of the sensitivity of sap flux to soil and plant variables assessed for an Australian woodland using a soil-plant-atmosphere model, Funct. Plant Biol., 35, 509–520, doi:10.1071/FP08114, 2008. 554

Full Screen / Esc

Printer-friendly Version

Interactive Discussion

Table 1. Key parameter values for the soil-plant-atmosphere model.

Parameter	Unit	Model value	SD	Derived
Foliar N	$gN m^{-2}$ leaf area	3.11	±0.22	measured
Stem conductivity	$mmol m^{-1} s^{-1} MPa^{-1}$	10	±2	estimated from K_{leaf}[*]
Minimum leaf water potential	MPa	−1.8	±0.1	measured
Leaf capacitance	$mmol m^{-2} MPa^{-1}$	3000		estimated[*]
Root resistivity	$MPa s g mmol^{-1}$	20	±10	estimated from K_{leaf}[*]
Rate constant for V_{cmax}	$\mu mol g N^{-1} s^{-1}$	31.4	±3	measured (A/Ci curves)
Rate constant for J_{max}	$\mu mol g N^{-1} s^{-1}$	60.6	±5	measured (A/Ci curves)
Leaf C	$gC m^{-2}$	122.4	±3.6	measured
Maximum root depth	m	1.2	±0.1	measured
Root biomass[a]	$gC m^{-2}$	120	±20	measured[*]
Sand	%	82 %	–	measured[*]
Clay[b]	%	10 %	–	measured[*]

[a] Root biomass to 50 % rooting depth.
[b] Increased from 2 % to 10 % due to otherwise poor water holding capacity of the soil.
[*] Adjusted during model parameterization; see Methods for details.

Table 2. Key parameter values for the carbon allocation-respiration part of the soil-plant atmosphere model.

Parameter	Description	Model value	Error	Derived
Cf	foliar C initial	72	±7.2	measured (interpolated)
Cw	Wood C initial	400	±80	measured (allometrics)
Cr	Fine root C initial	80	±20	measured (interpolated)
Clit	fresh fine litter C initial	20	±10	Williams et al. (2005)[*]
Csom	SOM C initial	5000	±500	measured (interpolated)
fa	fraction of GPP respired[a]	0.49		Williams et al. (2005)[*]
nf	NPP allocated to foliage	0.2		Williams et al. (2005)[*]
nrr	NPP allocated to fine roots	0.6		Williams et al. (2005)[*]
dc	turnover of litter to SOM	4.63×10^{-4} (90 d)		Williams et al. (2005)[*]
tf	turnover rate of foliage[b]	8.00×10^{-5} (1.4 yr)		measured[*]
tw	turnover rate of wood[c]	2.28×10^{-5} (5 yr)		Williams et al. (2005)[*]
tr	turnover rate of fine roots	1.67×10^{-4} (0.68 yr)		Andersen et al. (2008)
ml	mineralisation rate of litter	1.16×10^{-4} (1 yr)		Kelliher et al. (2004)
ms	mineralisation rate of SOM/CWD[d]	3.81×10^{-6} (30 yr)		Williams et al. (2005)[*]
tar	turnover rate of Ra pool	1.39×10^{-3} (30 d)		estimated[*]
resprate	Rh temperature response	0.044		measured[*]
aresprate	Ra temp response	0.025		measured[*] (leaf respiration)
gdtsum	bud expansion: GDS[e]	140		measured[*]

[a] Increased by 0.05 during winter (November–March).
[b] Turnover of 12 % needles in 60 d (September–October).
[c] Turnover of 20 % wood yr^{-1}.
[d] CWD (coarse woody debris).
[e] GDS (growing degree sum) = (gdd + avtemp – 5); starting 1 February (Hannerz, 1999)
[*] Adjusted during model parameterization; see Methods for details.

Table 3. Annual sums of net ecosystem exchange (NEE), gross primary productivity (GPP) and ecosystem respiration (Reco) derived from simulations with the SPA model (sim) and observations (obs) that were partitioned and gap-filled from measurements of net ecosystem exchange (available from March 2010).

	Year	−NEE	−GPP	Reco
		$(\mathrm{gC\,m^{-2}\,yr^{-1}})$		
sim	2010	174	888	714
sim	2011	221	958	737
obs	2011	242	850	608

Table 4. Treatment effects of increased precipitation compared to "normal" summer drought conditions on simulated annual gross primary productivity (GPP), net ecosystem exchange (NEE) and heterotrophic Rh (respiration) in 2010 and 2011. The treatment effect for soil water content (SWC) is provided for the watering period only. Precipitation treatments are in percent of water supplied to the irrigation experiment. Negative effects on NEE are depicted in bold.

Treatment	+Water (mm)	SWC	−GPP	−NEE	Rh	+Water (mm)	SWC	−GPP	−NEE	Rh
			2010 (%)					2011 (%)		
20 %	+87	+3	+0	**−2**	+1	+116	+13	+3	**−3**	+8
30 %	+131	+10	+2	**−5**	+6	+174	+43	+8	**−1**	+16
40 %	+175	+36	+5	**−1**	+9	+233	+65	+11	+5	+16
50 %	+218	+55	+8	+4	+10	+291	+73	+12	+7	+16
100 %	+436	+89	+9	+9	+11	+582	+96	+13	+9	+17

Table 5. Overview of the effects of climate scenarios on ecosystem fluxes in comparison to the 2010/11 conditions. The scenarios are: no summer precipitation, increased summer temperature and warming across all seasons (see Fig. 5). The larger effect between gross primary productivity (GPP) and heterotrophic respiration (Rh) is depicted in bold. Note that GPP is more affected by increases in summer temperature than reduced precipitation, confirming our first hypothesis. Considering our second hypothesis, we find a larger increase in Rh than GPP under the all seasons warming scenario, while changes in summer precipitation and temperature affected Rh less than GPP.

	Scenarios	T	−GPP	Rh	−NEE
			(%)		
−100 %	summer precipitation	−14	**−10**	−9	−12
+4.5 °C	summer temperature	−9	**−17**	−1	−38
+3/4.5 °C	all seasons temperature[*]	+3	+3	**+8**	−5

[*] September–May: +3 °C and June–August +4.5 °C
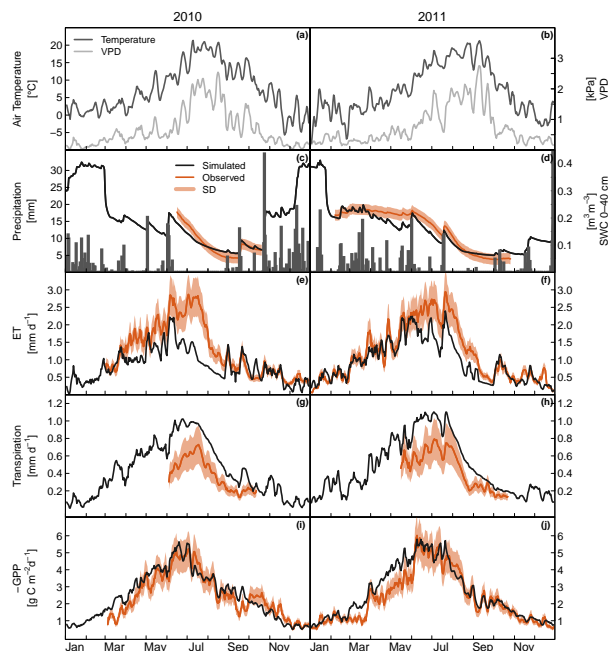
Fig. 1. Seasonality of daily meteorological conditions **(a–d)** and observed and simulated evapo-transpiration (ET), transpiration (*T*) and gross primary productivity (GPP, **e–g**) during 2010 and 2011. **(c–d)** Bars are sums of daily precipitation, and observed and simulated soil water content (SWC) are daily averages. Air temperature, vapor pressure deficit (VPD) and flux data are 5 day moving averages. Error estimates (SD) for observational data are given by the lighter colored areas around the mean. Note that observed transpiration fluxes do not include understory transpiration.
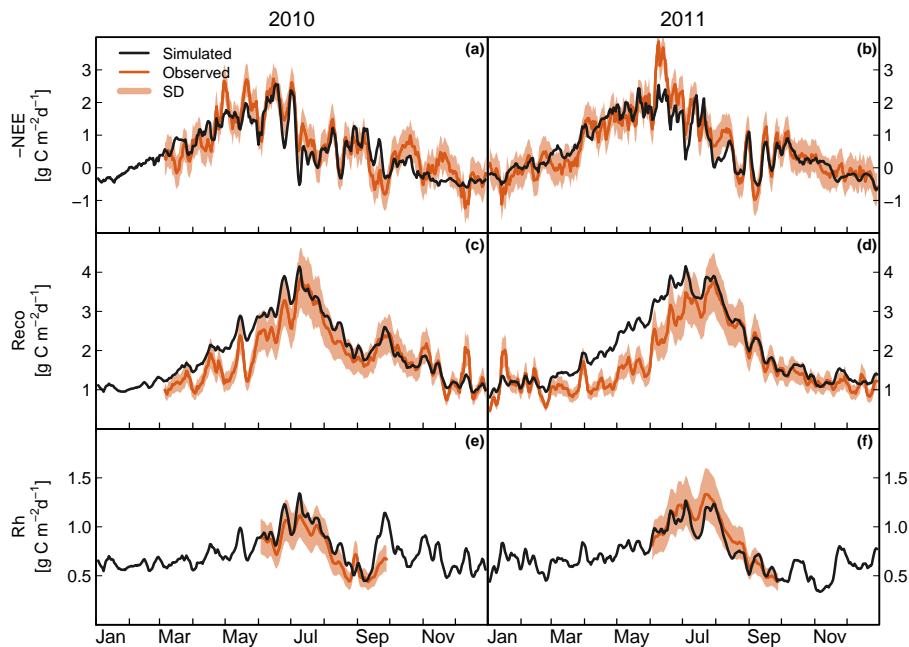
Fig. 2. Seasonality of observed and simulated daily net ecosystem exchange (NEE, **a–b**), ecosystem respiration (Reco, **c–d**) and heterotrophic respiration (Rh, **e–f**) in 2010 and 2011. Data are 5 day moving averages. Error estimates (SD) for observational data are given by the lighter colored areas around the mean.
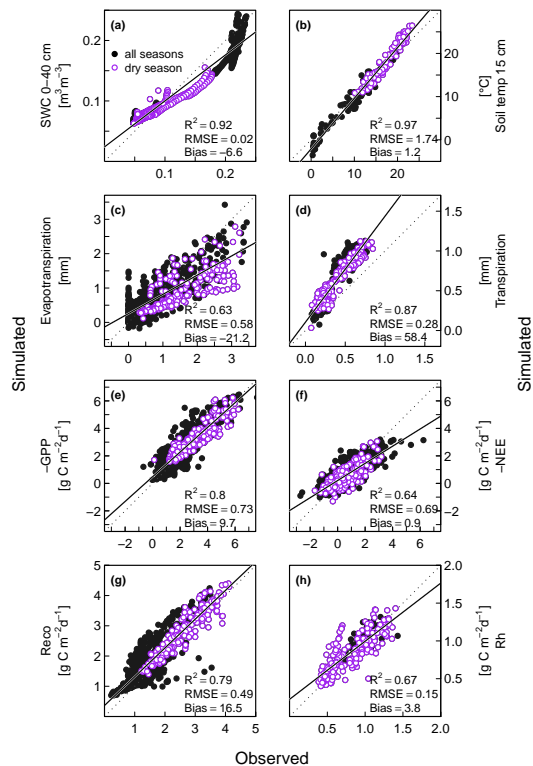
Fig. 3. Relationship between simulated and observed daily averages in 2010 and 2011. The regression between simulated and observed values for all seasons is provided by the solid line, and the R^2, RMSE (root mean square error) and percent mean bias are given. The dry seasons (July, August and September) are highlighted with the open circles (see legend), and the ideal one-to-one relationship is depicted by the dotted line.

Title Page

Abstract | Introduction

Conclusions | References

Tables | Figures

|◄ | ►|

◄ | ►

Back | Close

Full Screen / Esc

Printer-friendly Version

Interactive Discussion
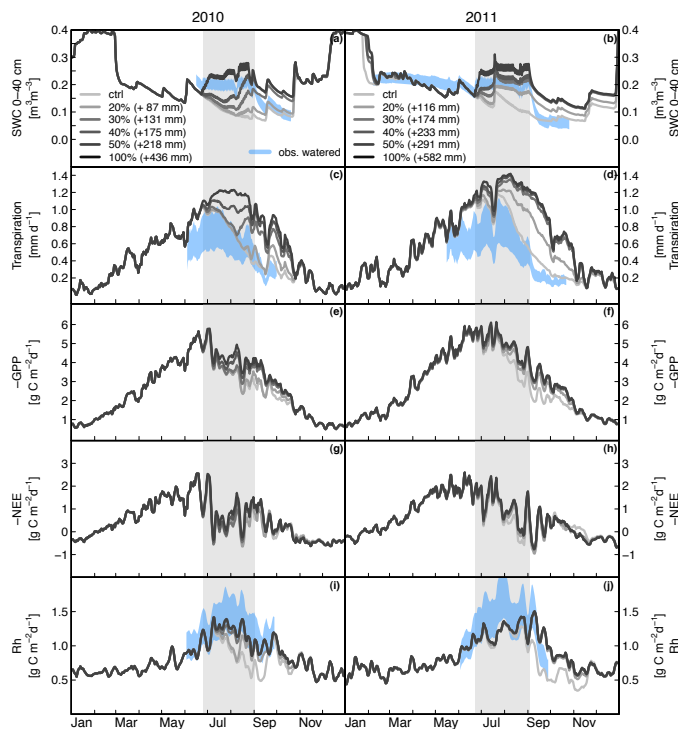
Fig. 4. Effects of increased summer precipitation on soil water content (SWC; **a–b**), transpiration (T; **c–d**) and carbon fluxes **(f–j)**. The amount of precipitation was step-wise increased from 20 % to 100 % of the irrigation water given to the watered treatment in summer 2010 and 2011. Observations of SWC, T and heterotrophic respiration (Rh) in the watered treatment are given by the light colored area (mean ± error estimate). The duration of the water additions is highlighted by the gray boxes. For a summary of the treatment effects see Table 4.

Title Page

Abstract | Introduction

Conclusions | References

Tables | Figures

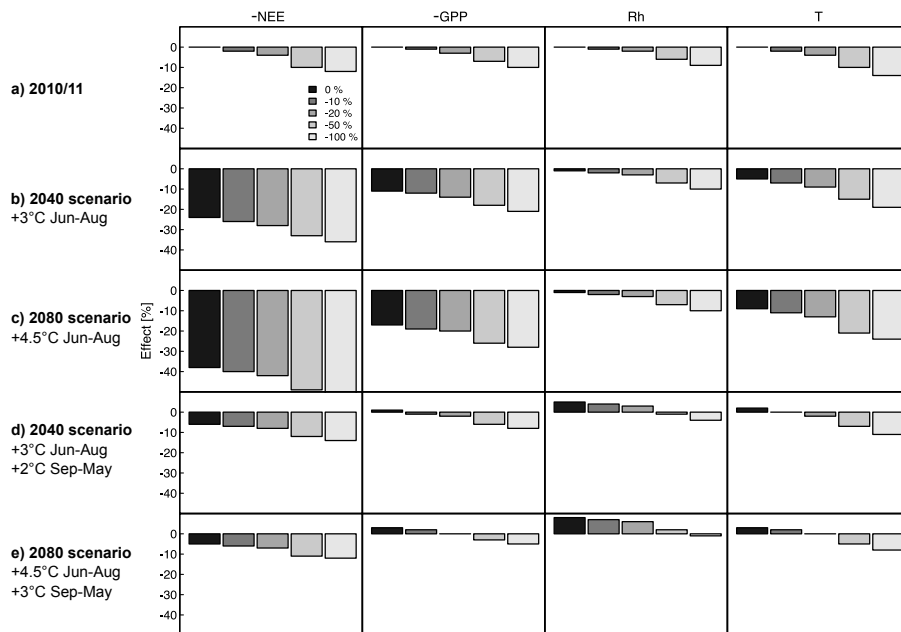|◀ | ▶|

◀ | ▶

Back | Close

Full Screen / Esc

Printer-friendly Version

Interactive Discussion

Fig. 5. Effects of reduced precipitation and increased temperatures on simulated ecosystem fluxes. Given are percent mean annual changes of the 10 yr model runs relative to the 2010/11 control conditions (0 % rain reduction). Precipitation from June to August was decreased by 0 %, 10 %, 20 %, 50 % and 100 % (10 % and 20 % reduction is in accordance to the climate scenarios for 2040 and 2080). **(a)** 2010/11 control temperature, **(b–c)** only summer temperature increased, **(d–e)** all seasons temperature increased. Note that CO_2 concentrations were 390 ppm for all scenarios.
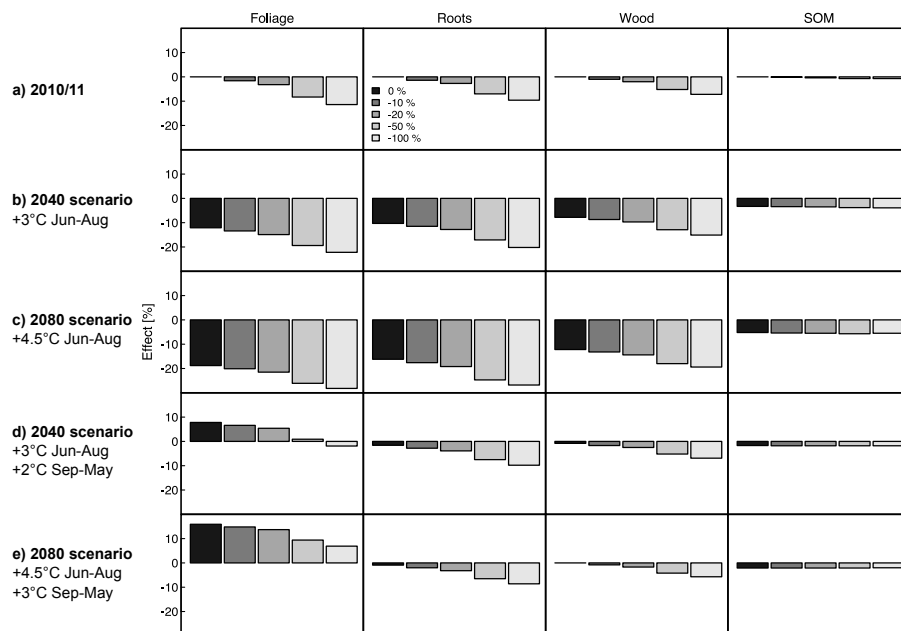
Fig. 6. Effects of reduced precipitation and increased temperatures on simulated biomass and soil organic matter (SOM). Given are percent mean annual changes of the 10 yr model runs relative to the 2010/11 control conditions (0 % rain reduction). Precipitation from June to August was decreased by 0 %, 10 %, 20 %, 50 % and 100 % (10 % and 20 % reduction is in accordance to the climate scenarios for 2040 and 2080). **(a)** 2010/11 temperature, **(b–c)** only summer temperature increased, **(d–e)** all seasons temperature increased. Note that CO_2 concentrations were 390 ppm for all scenarios.

Title Page

Abstract | Introduction

Conclusions | References

Tables | Figures
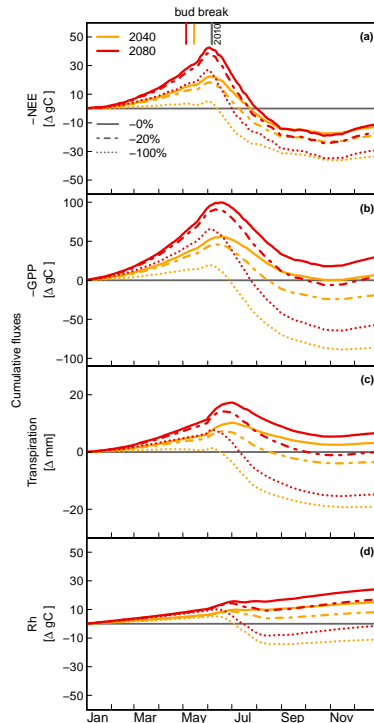
◀ | ▶

◀ | ▶

Back | Close

Full Screen / Esc

Printer-friendly Version

Interactive Discussion

Fig. 7. Seasonal course of anomalies in cumulative fluxes under future climate scenarios vs. 2010/11 conditions. Future scenarios are 2040 (June–Aug: +3 ˚C, September–May: +2 ˚C) and 2080 (June–August: +4.5 ˚C, September–May: +3 ˚C) with 0 %, 20 % or 100 % rain reduction during summer. The timing of bud break under the 2010/11, 2040 and 2080 simulations are depicted by the vertical lines. Note that CO_2 concentrations were 390 ppm for all scenarios.

Title Page

Abstract | Introduction

Conclusions | References

Tables | Figures

|◄ | ►|

◄ | ►

Back | Close

Full Screen / Esc

Printer-friendly Version

Interactive Discussion